Available online at www.sciencedirect.com
SCIENCE DIRECT
Applied Catalysis A: General 281 (2005) 129–137
APPLIED CATALYSIS A: GENERAL
www.elsevier.com/locate/apcata

Supercritical fluids and phase behavior in heterogeneous gas–liquid catalytic reactions

S. Pereda, S.B. Bottini, E.A. Brignole*

Planta Piloto de Ingeniería Química, PLAPIQUI-CONICET, Universidad Nacional del Sur, Camino La Carrindanga Km 7-CC 717, 8000 Bahia Blanca, Argentina

Received 12 August 2004; received in revised form 9 November 2004; accepted 15 November 2004
Available online 23 December 2004

Abstract

Gas–liquid catalyzed reactions carried out in a supercritical medium take advantage of the high reaction rates and improved selectivities that can be achieved by having reactants and products in a homogeneous phase. In this work, the phase behavior of several supercritical reactions are analyzed and the selection of adequate solvents is discussed. The reactions studied include the hydrogenation of terpenic compounds and unsaturated aldehydes, and the hydroformylation of hydrocarbons to produce aldehydes. Recent experimental results from the literature on the kinetics and selectivities of these reactions are discussed on the basis of the phase equilibrium scenario under the reaction conditions.

Keywords: Supercritical reaction media; Hydrogenation; Terpenes; Unsaturated aldehydes; Hydroformylation; 1-Hexene; Phase equilibria

1. Introduction

The history of reactions in supercritical media is relatively short. Subramanian and McHugh [1] give a comprehensive introduction to the subject. Savage et al. [2] present a wide variety of applications of supercritical fluids as reaction media. A special number of Chemical Review edited by Noyori covers different types of supercritical reactions, including the use of supercritical water, heterogeneous and homogeneous catalysis, biocatalysis, inorganic and organometallic systems and polymerization reactions.

In general, gas–liquid catalyzed reactions are diffusion-controlled. The use of supercritical fluids reduces this controlling step by eliminating the gas–liquid interface and by increasing the diffusivity of reactants. Therefore, reaction rates are greatly increased. In addition, better selectivity can be achieved in supercritical reactions due to the possibility of uncoupling process variables. For instance, while gas–liquid hydrogenation reactions require high temperatures to increase hydrogen solubility, the temperature of the supercritical process can be modified with no effects in compositions. This allows the selection of an operating temperature that improves selectivity without reducing conversion. Consequently, isomerization reactions favored by the lack of hydrogen at the catalyst surface can also be avoided. A good example of tuning operating conditions for the control of selectivity and conversion is given by Hitzler et al. [3] for the hydrogenation of *ortho*- and *meta*-cresol. Wandeler et al. [4] and Burk et al. [5] apply a supercritical media to perform enantioselective hydrogenations. Bhanage et al. [6] studied the hydrogenation of unsaturated aldehydes in supercritical CO_2 and obtained very high selectivities with a simple monometallic catalyst like Pt supported on alumina. The use of supercritical solvents has also a positive effect in the control of highly exothermic hydrogenation reactions due to the high heat capacity and thermal conductivity of these fluids. Other attractive properties of supercritical fluids for solid-catalyzed reactions are the low interfacial tensions and viscosities. Altogether, the favorable transport properties and the high

* Corresponding author. Tel.: +54 291 4861700x231; fax: +54 291 4861600.
E-mail address: ebrignole@plapiqui.edu.ar (E.A. Brignole).

0926-860X/$ – see front matter © 2004 Elsevier B.V. All rights reserved.
doi:10.1016/j.apcata.2004.11.019

reaction rates make the use of continuous supercritical reactors possible. Finally, the change of solvent power with temperature and pressure, typical of near-critical fluids, allows in many cases the in situ regeneration of the catalyst [7,8].

The conventional hydrogenation of liquids of low volatility is usually carried out in stirred batch reactors where a catalyst powder is intimately put in contact with the gas–liquid mixture (slurry reactors). In this type of process, the gas–liquid–solid reaction is controlled by the availability of hydrogen at the catalyst surface, which is limited by the low solubility of hydrogen and the high mass transfer resistance of the liquid phase. The use of an adequate supercritical fluid can bring the reactive mixture into homogeneous conditions, greatly increasing the reaction rate and selectivity. Härröd et al. [9] have studied experimentally the hydrogenation of heavy substrates, like vegetable oils and fatty esters, under supercritical conditions. These authors report an increase of several orders of magnitude in the reaction rate and improved selectivity, compared to conventional hydrogenation. Recently, Pereda et al. [10,11] applied phase equilibrium engineering tools to determine the process conditions required for the homogeneous supercritical hydrogenation of fatty esters and vegetable oils. Rovetto et al. [12,13] have presented experimental results on the phase equilibria of these systems.

In the hydroformylation of low molecular weight olefins, on the other hand, the Ruhrchemie/Rhone-Poulenc process (RR-PP), based on the use of a water-soluble catalyst, is commercially used. For substrates with a carbon number greater than 6 this process is not suitable due to the very low solubility of the olefin in the aqueous phase. In these cases, the catalyst is usually dissolved in an organic solvent (toluene or alkanes). The addition of a supercritical fluid avoids the use of organic solvents and drastically decreases the typical mass transfer limitation present in a gas–liquid catalyzed reaction [14,15].

The use of batch reactors is a common practice in bench scale experimental studies on supercritical reactions. However, the control of homogeneous conditions in these reactors is quite difficult. Baiker and co-workers [4,16] recommend the use of windows in the reaction vessels in order to control the phase conditions. Although in continuous reactors it is possible to have an independent control of process variables, the selection of pressure, temperature and composition should be carefully done to obtain the desired homogeneous state. Some recent experimental studies [17] make use of supercritical solvents but carry out the reactions under heterogeneous (gas–liquid) conditions. These authors claim that high concentrations of the supercritical solvent in the liquid phase increase mass transfer and hence reaction rates. Other authors [4,18] on the contrary, affirm that the system should be under homogeneous phase conditions in order to fully benefit from the advantages of working with a supercritical solvent. The knowledge of the phase behavior of a reaction process can help to understand the results of experimental studies and to plan and design experimental runs. This topic has been recently discussed by Grunwaldt et al. [19]; the experimental techniques applied in monitoring the phase behavior are extensively reviewed in this paper.

In the present work, the thermodynamic modeling and analysis of phase equilibria is applied to supercritical reactions. The results of some experimental studies reported in recent literature are analyzed and discussed in order to show the importance of being aware of the system phase state. The reactions studied covered the hydrogenation of α-pinene [20] and α,β-unsaturated aldehydes [6] and the hydroformylation of 1-hexene [21]. Before these reactions are discussed, it is first necessary to introduce some tools required for the analysis of the phase behavior of complex reactant mixtures and for the selection of an adequate supercritical solvent for a given reaction system.

2. Phase equilibria in supercritical reactors

The solvent to be used in a supercritical reaction should be non-reactive under process conditions. After this requirement is fulfilled, the critical temperature of the solvent is the primary property to take into account in the search of a suitable fluid to achieve homogeneous reaction conditions. The critical temperature of the solvent should be lower than the reaction temperature to assure complete miscibility of all gaseous reactants in the supercritical solvent. However, the critical temperature should not be far apart from the reaction temperature, to maintain the favorable properties of the near-critical state. In addition, the phase behavior of the binary mixtures between the solvent and the remaining reaction components should be investigated.

van Konynenburg and Scott [22] have shown that the fluid phase behavior observed in binary mixtures can be classified into five main types. In type I phase behavior, complete liquid miscibility is observed at all temperatures. When there is partial miscibility at low temperatures, the system is of type II. Type I behavior is usually found in systems with components of similar chemical nature and molecular size, like mixtures of hydrocarbons, noble gases or systems that do not deviate greatly from ideal behavior. Type II is typical of non-ideal mixtures of compounds of similar size, where non-ideality leads to liquid phase split at sub-critical conditions. When the immiscibility is persistent even at high pressures and temperatures, the systems are of type III. This behavior is characteristic, for example, of mixtures of CO_2 with high molecular weight alkanes and with vegetable oils. When the difference in molecular size becomes significant, in close to ideal systems, liquid–liquid immiscibility is observed near the solvent critical temperature, although complete miscibility is recovered at lower temperatures. This corresponds to type V behavior. Fig. 1 [23] is a master

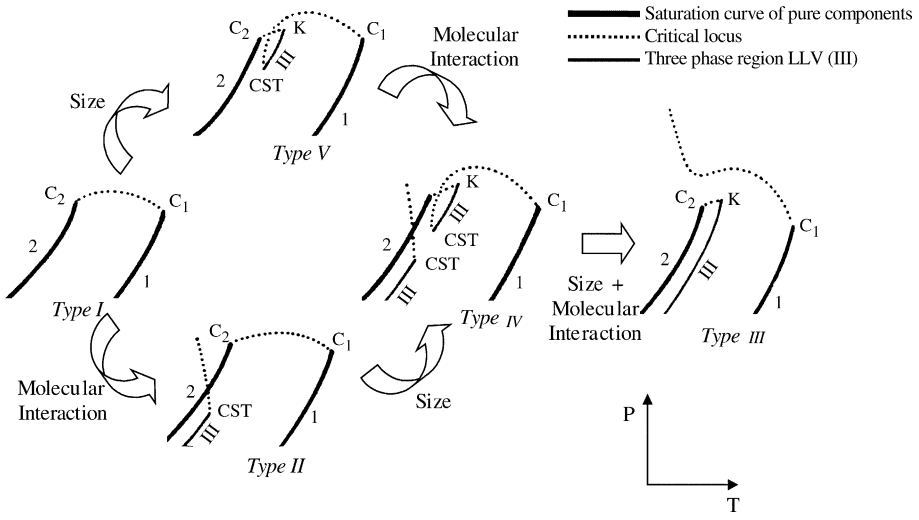

Fig. 1. Effect of molecular interactions and size differences in the types of binary fluid phase diagrams [23].

chart of the different types of binary fluid phase diagrams. The arrows in Fig. 1 indicate qualitatively the type of fluid phase behavior that can be expected when the components of the system under study exhibit greater molecular interactions, size differences or both.

Fig. 2 illustrates in more detail a type V phase diagram. The lines in this diagram indicate the boundaries of phase transitions and the critical locus. Also, the lower (L) and upper (U) critical end points are shown. This behavior is typical of mixtures of propane with triglycerides, such as sunflower oil [24] or tripalmitin [25]. Taking into account that the reaction temperatures will be above the critical temperature of the solvent, the operating pressure in these systems should be much higher than the critical pressure of the mixture in order to assure complete miscibility, i.e. the pressure should be above the $L_1 = L_2$ line.

In the search of an adequate supercritical solvent to achieve homogenous reaction conditions, two different approaches can be followed: (1) to compare the phase behavior of a given substrate with different solvents; (2) to follow the change in phase behavior of a given solvent with different families of chemical compounds. The first approach can only be applied to those chemical reactions where reactants and reaction products belong to the same or similar family of chemical compounds; for instance, in the hydrogenation of vegetable oils [11]. In the more general case, when reactants and reaction products are of different chemical nature, the second approach should be followed to take into account any possible change in the phase behavior as the reaction proceeds.

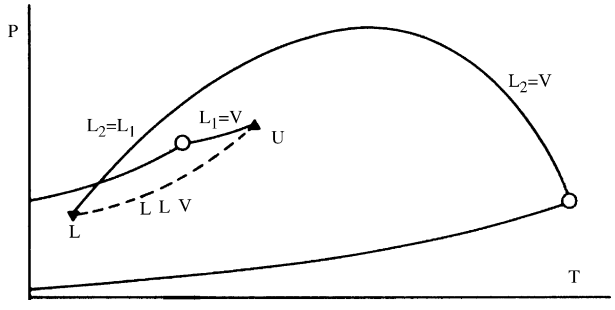

Fig. 2. Type V fluid phase diagram.

The liquid–liquid immiscibility of type V systems appears in many binary mixtures between supercritical solvents and organic substrates, beyond a given carbon number. Fig. 3 shows the regions of liquid–liquid immiscibility for binary mixtures of supercritical solvents (methane, ethane and propane) with hydrocarbons of different chain lengths [26]. On the other hand, Fig. 4 shows the liquid–liquid immiscibility domains for the systems (ethane + alcohols), (ethane + aromatic hydrocarbons) and (ethane + alkanes). It becomes clear from the last figure that ethane is not an adequate supercritical solvent for normal alcohols, because it presents liquid–liquid immiscibility even with methanol. However, ethane seems a better solvent for aromatic hydrocarbons or paraffins, because the

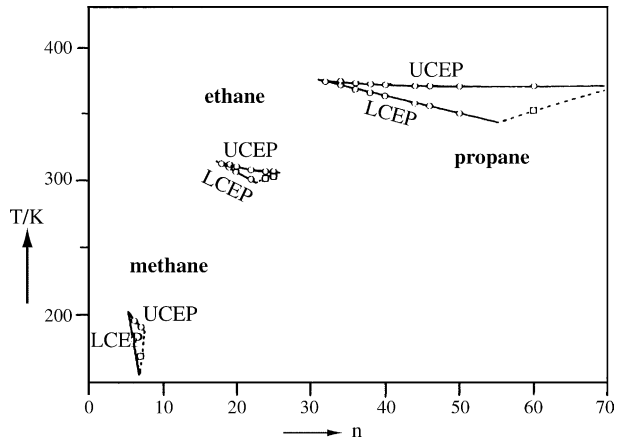

Fig. 3. Liquid–liquid immiscibility between supercritical solvents (methane, ethane and propane) and hydrocarbons with different carbon numbers (n). (○) Upper (UCEP) and lower (LCEP) critical end points [26].

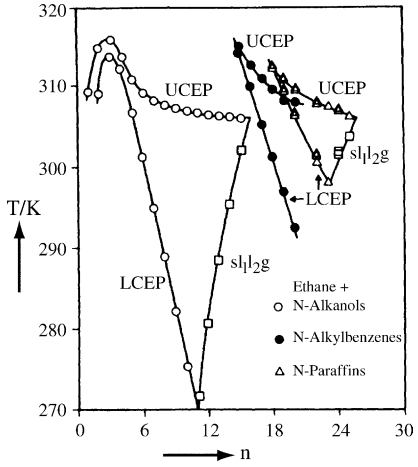

Fig. 4. Liquid–liquid immiscibility of ethane with *n*-alkanols, *n*-alkylbenzenes and *n*-alkanes. ○, ● and △ are upper and lower critical end points of *n*-alkanols, *n*-alkylbenzenes and *n*-alkanes, respectively [26].

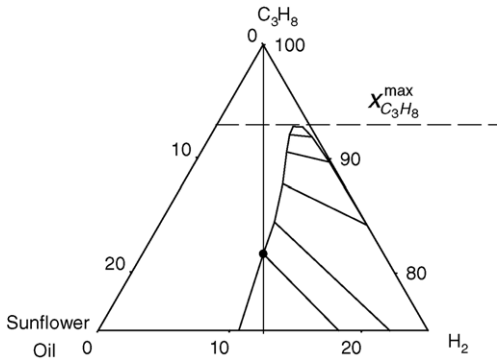

Fig. 5. Binodal curve for the hydrogenation of sunflower oil at 373 K and 12 MPa. $x^{max}_{C_3H_8}$ represents the minimum concentration of propane that guarantees homogenous operation at any H_2/oil ratio.

liquid–liquid immiscibility appears at carbon numbers greater than 15 or 18, respectively.

Carbon dioxide has been the most studied solvent for supercritical reactions. However, it depicts strong liquid–liquid and gas–liquid immiscibility for hydrocarbons with carbon numbers greater than 13. In addition, CO_2 presents a rather low critical temperature for reactions carried out at moderate or high temperatures. Unfortunately, the type of data shown in Figs. 3 and 4 are only known for a limited number of families of organic compounds with some supercritical solvents. Therefore, there is a need of reliable thermodynamic models to explore the possible phase scenarios found in mixtures between reacting components and supercritical solvents. Group contribution equations of state, such as MHV2 [27,28], and GCA-EoS [29] are particularly useful to represent the complex phase behavior observed in these asymmetric reactive mixtures. When both, the mixture between reactants and reaction products are ternary systems, then ternary phase diagrams can be used to determine the boundaries of the homogeneous region at the reactor temperature and pressure. When the number of components of the reacting system is greater than 3, the best way to describe the one-phase boundaries is by using a phase envelope (pressure versus temperature) diagram. For each composition (i.e. for each degree of conversion), this diagram gives the bubble and dew point lines, as well as the critical point of the mixture [30]. In both types of diagrams it is possible to follow the changes in the one-phase boundaries as the reaction proceeds. The operating variables can thus be selected so as to avoid entering the heterogeneous region. Pereda [11] discusses the use of these diagrams in two typical examples: the hydrogenation of vegetable oils (Fig. 5) and the hydrogenolysis of fatty acid methyl esters (Fig. 6) under supercritical propane. The phase boundaries in these diagrams have been predicted by the GCA-EoS equation of state.

In the present work, two hydrogenation reactions were studied: the hydrogenation of α-pinene to pinane and that of unsaturated aldehydes to the corresponding alcohols. The phase equilibrium conditions of these systems were calculated with the MHV2 group contribution equation of state [31]. The model requires information on the critical properties and acentric factor of pure components. Since there is no experimental information on the critical properties of the liquid substrates studied in this work, these properties were estimated with a group contribution method. The critical properties shown in Table 1 were predicted with Jobak's method [32]. The normal boiling temperature required to calculate the critical temperature were taken from Aldrich catalog of fine chemicals. Finally, the acentric factor was computed by definition, using the Lee–Kesler relation for vapor pressures [32].

3. Hydrogenation of α–pinene

The hydrogenation of α-pinene to pinane (Fig. 7) is the first step in the process of converting an economic and

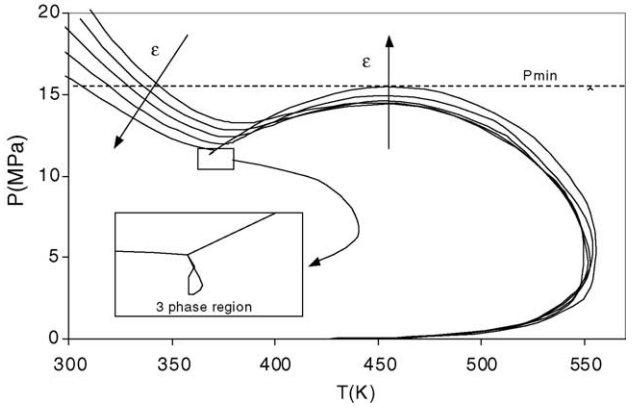

Fig. 6. Phase envelopes for the hydrogenolysis of methyl palmitate. Conversion: $0 \leq \varepsilon \leq 1$. P_{min} is the minimum pressure required for homogeneous operation at normal working temperatures.

Table 1
Predicted critical properties and acentric factor of some terpenic compounds

Compound	T_b (K)	T_c (K)	P_c (MPa)	ω
α-Pinene	429.29	644.00	2.76	0.2209
Pinane	441.15	636.45	2.73	0.3827
Cinnamaldehyde	524.15	765.54	3.78	0.4628
Cinnamyl alcohol	530.65	735.28	3.87	0.5838

versatile raw material into a variety of products of high-added value.

Chouchi et al. [20] have studied the hydrogenation of α-pinene under supercritical CO_2 in a batch reactor operating at 323 K and 14 MPa with a Pd/C catalyst. They showed that the reaction rate and conversion are low when the reactor operates under homogenous conditions. On the contrary, better conversions were achieved when the CO_2 pressure was decreased, even though the system became heterogeneous.

In order to explain these apparently contradictory results, the MHV2 model was used to explore the phase equilibrium scenario of the reactive system. Chouchi et al. [20] do not report the composition of the reactive mixture, but they explain clearly how the batch reactor was fed: first they introduced the catalyst together with 1 g of α-pinene; then they pressurized the system with CO_2 up to the desired pressure (8, 9, 10 or 12 MPa); and finally they fed H_2 until a total pressure of 14 MPa was reached. With this information and knowing also the total volume of the reactor (40 cm^3), it was possible to estimate the composition of the reactive system using the Peng–Robinson equation of state (PR-EoS) with classical mixing rules to calculate molar densities (the PR-EoS model is known to give better density predictions than the Soave–Redlich–Kwong equation). The calculation is done in two iterative steps:

(a) Since the number of moles of the liquid substrate is known ($n_{substrate}$), the first step is an iterative process to determine the number of CO_2 moles (n_{CO_2}) in the reactor: (1) the initial number of moles n_{CO_2} is guessed; (2) the molar volume (V_1) of the mixture at the feeding temperature and intermediate pressure (8, 9, 10, or 12 MPa) is calculated with the PR-EoS equation. The iterative process stops when $(n_{substrate} + n_{CO_2}) \times V_1$ equals the total volume of the reactor.
(b) The second iterative process gives the amount of H_2: (1) the initial number of H_2 moles (n_{H_2}) is guessed; (2) the PR-EoS equation is used to calculate the molar volume (V_2) of the mixture ($n_{substrate} + n_{CO_2} + n_{H_2}$) at the feeding temperature and final pressure (14 MPa). Again, the iterative process stops when $(n_{substrate} + n_{CO_2} + n_{H_2}) \times V_2$ equals the total volume of the reactor.

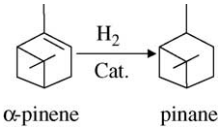

Fig. 7. Hydrogenation of α-pinene.

If the feeding composition corresponds to a two-phase region, the total volume is calculated taking into account the molar volumes of the two coexisting phases: $n_L \times V_L + n_V \times V_V = V_{reactor}$.

For each experimental run carried out by Chouchi et al. [20], Fig. 8 shows the phase envelopes calculated with the MHV2 model. The lines represent predictions for both, the initial composition of the reactive mixture (full line) and the composition after complete conversion (dashed line). The dot represents the operating temperature and pressure of the reactor.

In agreement with the experimental observation, the MHV2 model predicts one-phase operating conditions at CO_2 initial pressures higher than 10 MPa (Fig. 8(c) and (d)). At 8 MPa the reactive mixture is biphasic all along the reaction path (Fig. 8 (a)). According to the MHV2 predictions, at 9 MPa the system goes from homogeneous conditions at zero conversion, to the two-phase limit at complete conversion (Fig. 8(b)).

The triangular diagram of Fig. 9 shows the binodal curves of the reactants (H_2 + α-pinene + CO_2) and reaction products (H_2 + pinane + CO_2) at 323 K and 14 MPa, together with the experimental feed compositions. It becomes clear from this figure that, in order to achieve complete miscibility, a very high dilution of the reactive mixture is required, which in turn produces low reaction rates. In this case, the solvent and/or the selected operating conditions were not the most favorable. A possible reaction path that could give higher reaction rates working under homogeneous conditions is indicated in Fig. 9 (⇒).

4. Hydrogenation of α,β-unsaturated aldehydes

Unsaturated aldehydes can be transformed into unsaturated alcohols by selective hydrogenation of the aldehyde functional group (Fig. 10). It is difficult to achieve high selectivity in this process, because double bonds hydrogenate more easily than carbonyl groups, producing saturated alcohols and aldehydes as byproducts.

Bhanage et al. [6] studied the supercritical hydrogenation of three α,β-unsaturated aldehydes (cinnamaldehyde, crotonaldehyde and α-methyl-*trans*-cinnamaldehyde) under supercritical CO_2. The experimental work was carried out in a batch reactor operating at 323 K, with a Pt/Al_2O_3 catalyst. The authors analyzed the effect of the total and partial pressures of H_2 and CO_2, in the selectivity of the reaction. Previous work on this field shows that the use of monometallic catalysts supported on Al_2O_3 lead mostly to the formation of saturated aldehydes [33]. However, Bhanage et al. [6] reach very high selectivities towards the unsaturated alcohol when the reaction is carried out under supercritical CO_2. These authors get selectivities up to

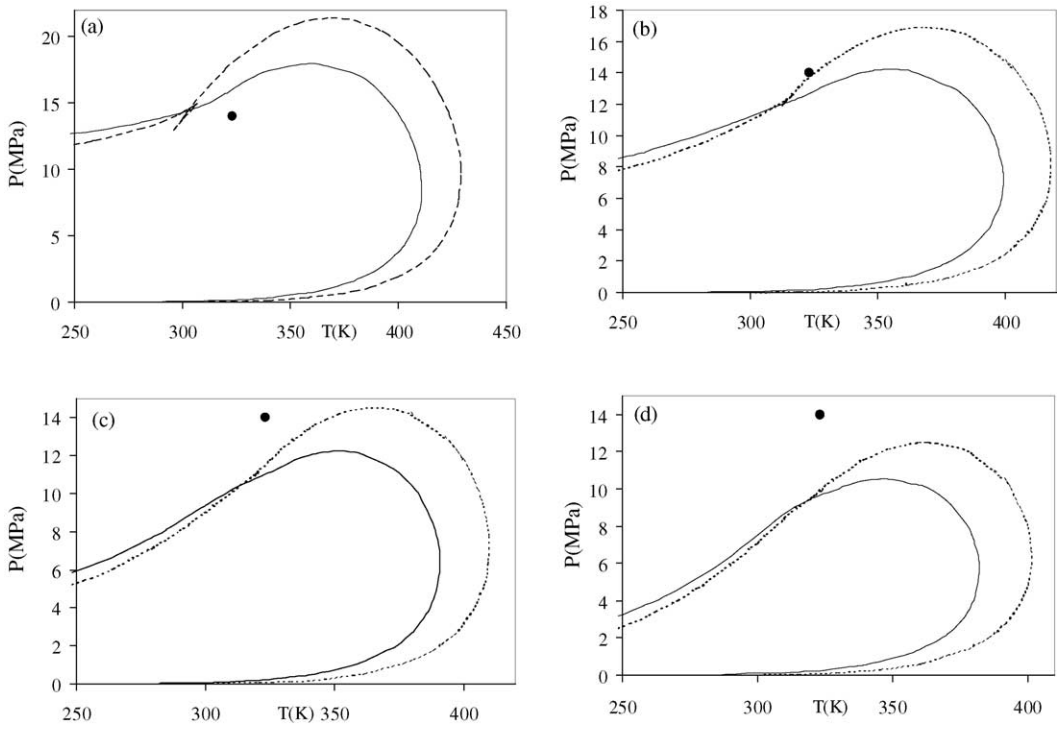

Fig. 8. Hydrogenation of α-pinene. Phase envelopes: (a) $P_{CO_2} = 8$ MPa; (b) $P_{CO_2} = 9$ MPa; (c) $P_{CO_2} = 10$ MPa; (d) $P_{CO_2} = 12$ MPa. (●) Chouchi et al. [20] experimental operating conditions (323 K and 14 MPa); lines are MHV2 predictions; (—) conversion $x = 0\%$; (– – –) conversion $x = 100\%$.

70 and 96% in the crotonaldehyde and cinnamaldehyde hydrogenation, respectively. They also point out the specific role of CO_2 in achieving high selectivities for the hydrogenation of unsaturated aldehydes.

Fig. 11 shows the MHV2 phase equilibrium predictions for the binary systems cinnamaldehyde + CO_2 and cinnamyl alcohol + CO_2, at high CO_2 molar fractions. As expected, the alcohol is less soluble in CO_2, due to the non-ideality produced by association effects. To compare experiments carried out at different total pressures on a single diagram, the experimental conditions were projected on a binary (solvent + substrate) diagram. Consequently, the compositions of the experimental runs in Fig. 11 are given on a H_2-free molar basis. If an experimental point lies in the binary two-phase region, then the ternary system $H_2 + CO_2$ + substrate will be heterogeneous. However, no direct connection can be withdrawn between the binary and ternary phase behavior, if the experimental point lies in the homogeneous region.

Fig. 11 shows that six of the experimental runs were carried out at heterogeneous conditions, in agreement with the low conversions obtained (lower than 35%). Higher conversions and selectivity are achieved when the system goes into the homogeneous region. This shows another advantage of phase equilibrium engineering: it can save time and money in the lab. A previous exploration of the phase boundaries would have discarded the last six runs shown in Fig. 11.

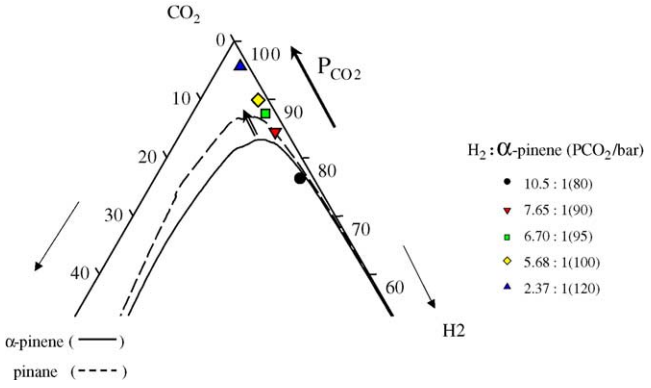

Fig. 9. Hydrogenation of α-pinene. Triangular phase diagram at 323 K and 14 MPa. Binodal curves: MHV2 predictions; dots: experimental compositions; ⇒: alternative reaction path.

5. Hydroformylation of 1-hexene

The hydroformylation reaction is the addition of synthesis gas (CO and H_2) to alkenes, with the aim to synthesize aldehydes. Marteel et al. [21] studied the hydroformylation of 1-hexene to produce heptanal under supercritical CO_2. The experimental work was performed in a batch reactor at 373 K and 18.6 MPa using a platinum–phosphine complex as catalyst and $SnCl_2{\cdot}2H_2O$ as co-catalyst. They report that no side hydrogenation reaction occurred and that high selectivity towards linear heptanal was obtained.

For this reacting system, the MHV2 model was not able to give a good representation of the phase equilibrium

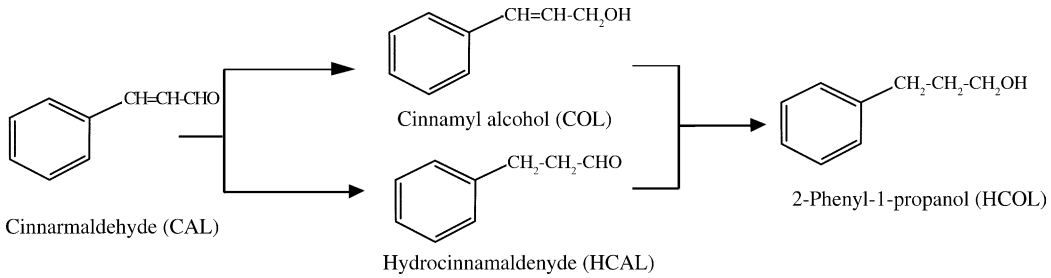

Fig. 10. Possible reaction paths for the hydrogenation of α,β-unsaturated aldehydes.

experimental data available in the literature [34]. For this reason, the GCA-EoS equation was applied (Appendix A).

Jiang et al. [34] measured bubble pressures at constant compositions, for different mixtures of the whole reactive system (reactants + products + solvent). Starting with two different mixtures between reactants and solvent (representing two possible feed compositions to a reactor), and following the change in composition as the reaction proceeds, Jiang et al. [34] prepared several mixtures representative of those obtained at different conversions (x = 0, 25, 50, 75, 90 and 100%). Fig. 12 shows Jiang's data together with GCA-EoS predictions, for a mixture with an initial composition (on a molar basis) of H_2:CO:1-hexene = 1:1:1 and CO_2 = 0.724. As it can be seen, the model is able to accurately predict the phase behavior of this system.

As the conversion increases, the system changes from a H_2 + CO-like behavior to a CO_2-like behavior. This means that at high H_2 + CO concentrations the bubble pressure of the mixture decreases with temperature; however, when H_2 and CO are consumed, the bubble pressure of the system increases with temperature. Jiang's data show how important it is to study the phase behavior of the whole reacting system and to follow all possible changes as the reaction proceeds. For example, for the feed composition shown in Fig. 12, at the higher temperatures the maximum pressure is attained at intermediate conversions. This means that, if the reaction is carried out at temperatures above 320 K, it is necessary to apply a pressure greater than the bubble pressure of the feed mixture in order to attain homogeneity. Even though there is a consumption of H_2 and CO, the bubble pressure of the system increases for conversions up to 50%. On the other hand, if the reaction is performed at temperatures below 320 K, by applying a pressure equal to the bubble pressure of the feed mixture, the reaction mixture will remain at homogenous conditions within all the conversion range. This information is of main importance to make a correct optimization of the process operating conditions.

With the aim to analyze the selection of process conditions done by Marteel et al. [21], the feasible operating region for the hydroformylation of 1-hexene at 373 K under supercritical CO_2 was determined (see full line in Fig. 13). This line represents the minimum amount of solvent required to ensure homogenous operation, given by the solvent/reactants feed ratio R (kg solvent/kg reactants) as a function of the operating pressure. This solvent requirement was calculated following the phase equilibrium engineering criteria applied by Pereda et al. [10] for the supercritical hydrogenation of fatty esters. The cross symbol in Fig. 13 represents the operating conditions used by Marteel et al.,

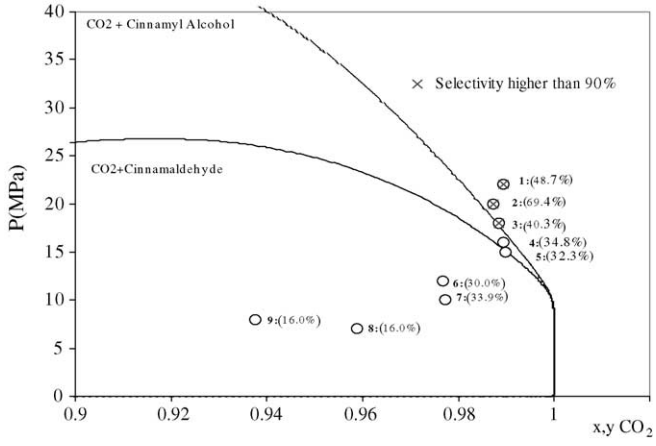

Fig. 11. Hydrogenation of cinnamaldehyde. Binary phase diagrams at high CO_2 mole fractions. Lines: MHV2 predictions; dots: conditions of experimental runs; compositions of these points are feed compositions on a H_2-free molar basis; values within brackets are conversions of the reaction.

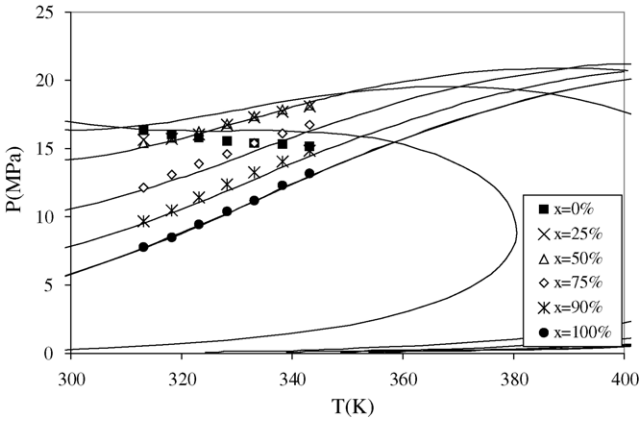

Fig. 12. Bubble pressures of the system H_2 + CO + CO_2 + 1-hexene + heptanal. Initial composition (conversion x = 0%): H_2:CO:1-hexene = 1:1:1 and CO_2 = 0.724 (molar basis). Dots: experimental data [34]. Lines: GCA-EoS predictions.

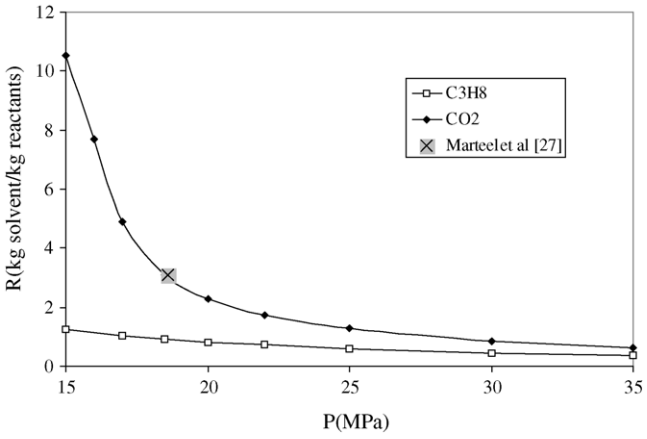

Fig. 13. Feasible operating conditions for the hydroformylation of 1-hexene at 373 K using CO_2 and propane as supercritical solvents.

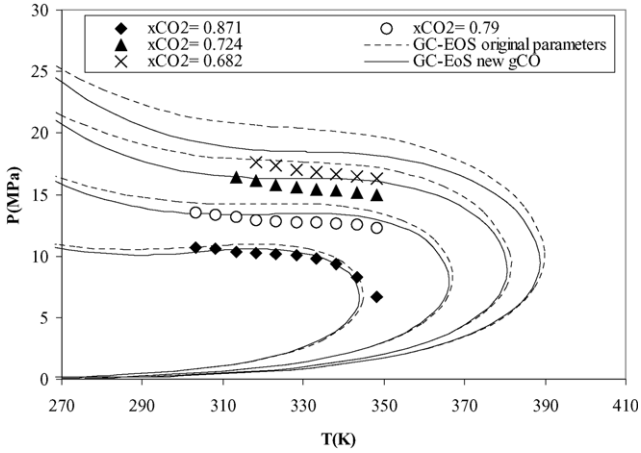

Fig. 14. Bubble pressures of the quaternary system $H_2 + CO + CO_2$ + 1-hexene. H_2:CO:1-hexene = 1:1:1. Experimental data: Jiang et al. [34]. Dashed lines: GCA-EoS predictions with original parameters. Full lines: GCA-EoS correlation.

which lie just on the limit of the operating region predicted by the GCA-EoS model.

In order to compare the performance of CO_2 with an alternative solvent, the phase equilibrium calculations were repeated for mixtures of propane with the same reaction system. Following the same procedure, the amount of propane required to attain homogeneous conditions was determined. The results are represented by the dashed line in Fig. 13. From this figure, we can conclude that the value of the operating pressure determines whether it is more convenient to use CO_2 or propane. For instance, at pressures higher than 25 MPa there is no important decrease in solvent requirement if CO_2 is changed by propane. Hence, CO_2 becomes the best solvent due to its well-known favorable properties (low cost, not flammable, not toxic, etc.). On the other hand, when the operating pressure is below 20 MPa, the use of propane represents a great reduction in solvent requirement. For example, at the operating pressure used by Marteel et al. [21] (18.6 MPa), the amount of propane required is three times lower than that of CO_2. Moreover, for a pressure of 15 MPa, this reduction is of one order of magnitude. In conclusion, the use of propane can represent an important reduction of process operating costs.

Many authors [35–37] affirm that the heterogeneous operation of a supercritical reactor is a better option than a homogeneous operation. The attainment of higher reaction rates in supercritical fluids, as compared to traditional liquid solvents, leads them to the conclusion that the solubility of H_2 increases due to the presence of a liquid phase 'expanded' by the supercritical fluid. This is not generally true. There is very little increment in the solubility of hydrogen in the liquid phase. Reaction rates may increase due to the better transport properties of this expanded liquid phase, but the solubility problem remains almost unchanged. For this reason, there is not such a drastic increase in the reaction rates of the two-phase supercritical processes, like the one obtained by working at adequate one-phase conditions [9].

6. Conclusions

The use of phase equilibrium engineering tools gives a good understanding of the supercritical reaction processes. In this work, the MHV2 equation was applied to analyze the hydrogenation of α-pinene and cinnamaldehyde. In the case of hydroformylation of 1-hexene, the GCA-EoS model was applied and a feasible operating region for two different supercritical solvents was determined. The results show that overlooking phase equilibrium considerations may lead to wrong conclusions regarding the results obtained in experimental studies.

Appendix A.

The experimental data measured by Jiang et al. [34] was used to fit GCA-EoS model parameters and to test the model predictive capability. After checking the quality of the predictions, the model was used to analyze the selection of a supercritical solvent for the hydroformylation of 1-hexene and to predict the feasible operating region to attain homogeneity. The GCA-EoS model has three contributions to the residual Helmholtz energy (A_R): repulsive or free volume, attractive and associative contributions. A complete description of the model was presented by Gros et al. [29] and updated by Ferreira [38]. The attractive part of A_R is a group contribution version of a density-dependent NRTL expression, in which the attractive energy parameter (g_{ij}) takes into account the interactions between functional groups. The energy parameter g_{ij} is calculated using three pure group parameters (g^*_{ii}, g'_{ii} and g''_{ii}), generally obtained from pure component vapor pressure data, and four binary interaction parameters: the symmetrical binary parameters k^*_{ij} and k'_{ij} and the asymmetrical non-randomness parameters α_{ij} and α_{ji}, which are fitted to binary phase equilibrium experimental data.

The dashed lines in Fig. 14 show the GCA-EoS predictions of bubble points for the system H_2 + CO + CO_2 + 1-hexene, using the original set of parameters. As it is shown, the model predicts higher bubble pressures than the corresponding experimental data. This type of error in a gas–liquid system can be associated with a wrong extrapolation of the gas vapor pressures at temperatures higher than its critical point. Since H_2 has an extremely low critical point, its pure group parameters were obtained by fitting not only vapor pressure data, but also phase equilibrium data at higher temperatures. However, in the case of CO, the original parameters were fitted only to CO vapor pressure data. This means that the energy parameters for CO (critical temperature = 132.9 K) are being extrapolated around 200 K to reach the temperatures covered in Jiang's data. The experimental data shown in Fig. 14 were used to fit a new set of energy parameters for the CO functional group. Keeping the original value for the temperature independent parameter ($g^*_{ii} = 309,610$), two new temperature-dependent parameters g'_{ii} and g''_{ii} were determined. The best fit of the experimental data (see full lines in Fig. 14) was obtained with the following values: $g'_{ii} = 0.25$, $g''_{ii} = -0.37$.

Jiang et al. [34] also measured bubble pressures of the complete reacting system (reactants + products + solvent). These data were used to test the predictive capability of the model. The results of the predictions are presented in the Section 5 (Fig. 12).

References

[1] B. Subramanian, M.A. McHugh, Ind. Eng. Chem. Proc. Des. Dev. 25 (1986) 1–12.
[2] P. Savage, S. Gopalan, T. Mizan, C. Martino, E. Brock, AIChE J. 41 (1995) 1723–1778.
[3] M.G. Hitzler, F.R. Smail, S.K. Ross, M. Poliakoff, Org. Proc. Res. Dev. 2 (1998) 137–146.
[4] R. Wandeler, N. Künzle, M.S. Schneider, T. Mallat, A. Baiker, J. Catal. 200 (2000) 377–388.
[5] M.J. Burk, S. Feng, M.F. Gross, W. Tumas, J. Am. Chem. Soc. 117 (1995) 8277–8278.
[6] B.M. Bhanage, Y. Ikushima, M Shirai, M. Arai, Catal. Lett. 62 (1999) 175–177.
[7] B. Subramaniam, Appl. Catal. A: Gen. 212 (2001) 199–213.
[8] H. Tiltscher, H Hofmann, Chem. Eng. Sci. 42 (1987) 959–977.
[9] M. Härröd, S. van den Hark, A. Holmqvist, P. Moller, Proceedings of the Fourth ISSAF International Symposium on High Pressure Process Technology and Chemical Engineering, Venice, Italy, 2002.
[10] S. Pereda, S.B. Bottini, E.A. Brignole, AIChE J. 48 (2002) 2635–2645.
[11] S. Pereda, Ingeniería del Equilibrio entre Fases: Aplicación a Reactores de Hidrogenación Supercrítica, Ph.D. Thesis, Universidad Nacional del Sur, Bahía Blanca, Argentina, 2003.
[12] L.J. Rovetto, S.B. Bottini, E.A. Brignole, C.J. Peters, J. Supercrit. Fluids 25 (2003) 165–176.
[13] L.J. Rovetto, S.B. Bottini, C.J. Peters, J. Supercrit. Fluids 31 (2004) 111–121.
[14] A.R. Tadd, A. Marteel, M.R. Mason, J.A. Davies, M.A. Abraham, Ind. Eng. Chem. Res. 41 (2002) 4514–4522.
[15] A.R. Tadd, A. Marteel, M.R. Mason, J.A. Davies, M.A. Abraham, J. Supercrit. Fluids 25 (2003) 183–196.
[16] A. Baiker, Chem. Rev. 99 (1999) 453–473.
[17] B. Subramaniam, C.J. Lyon, V. Arunajatesan, Appl. Catal. B: Environ. 37 (2002) 279–292.
[18] S. van den Hark, M. Härröd, Ind. Eng. Chem. Res. 40 (2001) 5052–5057.
[19] J.-D. Grunwaldt, R. Wandeler, A. Baiker, Catal. Rev. 45 (2003) 1–96.
[20] D. Chouchi, D. Gourgouillon, M. Courel, J. Vital, M. Nunes da Ponte, Ind. Eng. Chem. Res. 40 (2001) 2551–2554.
[21] A. Marteel, J.A. Davies, M.R. Mason, T. Tack, S. Bektesevic, M.A. Abraham, Catal. Commun. 4 (2003) 309–314.
[22] P.H. van Konynenburg, R.L. Scott, Phil. Trans. 298 (1980) 495–540.
[23] K.D. Luks, Fluid Phase Equilib. 29 (1986) 209–224.
[24] J.C.B. de la Fuente, G.D. Mabe, E.A. Brignole, S.B. Bottini, Fluid Phase Equilib. 101 (1994) 247–257.
[25] H.G.A. Coorens, C.J. Peters, J. De Swaan Arons, Fluid Phase Equilib. 40 (1988) 135–151.
[26] C.J. Peters, in: E. Kiran, M.H. Levelt Sengers (Eds.), Multiphase Equilibria in Near-critical Solvents, Kluwer Academic Publishers, 1994.
[27] M.L. Michelsen, Fluid Phase Equilib. 60 (1990) 42–58.
[28] M.L. Michelsen, Fluid Phase Equilib. 60 (1990) 213–219.
[29] H.P. Gros, S.B. Bottini, E.A. Brignole, Fluid Phase Equilib. 116 (1996) 537–544.
[30] M.L. Michelsen, Fluid Phase Equilib. 4 (1980) 1–10.
[31] S. Dahl, M.L. Michelsen, AIChE J. 36 (1990) 1829–1836.
[32] R.C. Reid, J.M. Prausnitz, B.E. Poling, The Properties of Gases and Liquids, 4th ed. McGraw-Hill, USA, 1987.
[33] M. Consonni, D. Jokic, D. Murzin, R. Touroude, J. Catal. 188 (1999) 165–175.
[34] T. Jiang, H. Zhenshan, H. Buxing, G. Liang, L. Zhimin, H. Jun, Y. Guanying, Fluid Phase Equilib. 215 (2004) 85–89.
[35] L. Devetta, A. Giovanzana, P. Canu, A. Bertucco, B.J. Minder, Catal. Today 48 (1999) 337–345.
[36] A. Bertuco, P. Canu, L. Devetta, A.G. Zwahlen, Ind. Eng. Chem. Res. 36 (1997) 2626–2633.
[37] H-S. Phiong, F.P. Lucien, A.A. Adesina, J. Supercrit. Fluids 25 (2003) 155–164.
[38] O. Ferreira, Modelling of association effects by group-contribution: application to natural products, Ph.D. Thesis, Univ. de Porto, Porto, Portugal, 2003.